Inorg. Chem. **2004**, *43*, 822–829

Synergic Nitrogen Source Route to Inorganic Fullerene-like Boron Nitride with Vessel, Hollow Sphere, Onion, and Peanut Nanostructures

Fen Xu, Yi Xie,* Xu Zhang, Shuyuan Zhang, Xianming Liu, and Xiaobo Tian

Structure Research Lab, Department of Chemistry, University of Science & Technology of China, Hefei, Anhui 230026, People's Republic of China

Received July 24, 2003

In this paper we describe the large-scale synthesis of inorganic fullerene-like (IF-like) hexagonal boron nitride with vessel, hollow sphere, peanut, and onion structures by reacting BBr_3 with the synergic nitrogen sources $NaNH_2$ and NH_4Cl at 400–450 °C for 6–12 h. The composition of products could be confirmed to be pure boron nitride with hexagonal structures by the XRD patterns and FT-IR, XPS, and EDXA spectra. The representative HRTEM images clearly reveal the layerlike features of the products. Here, the peanut-like structure of the IF-like BN is reported for the first time, and added to the list as one kind of new morphology of BN nanomaterials. The similarity in the structure between *h*-BN and graphite is responsible for the formation of IF-like BN with nanostructures of vessels, hollow spheres, peanuts, and onions.

Introduction

Since the discovery of C_{60}[1] and carbon nanotubes,[2] various fullerene-like (abbreviated as IF-like) structures of carbon families have been widely reported such as nanocapsules[3] and closed spherical carbon shells.[4] They also opened up a new challenging era in chemistry, solid-state physics, materials science, and nanoscale engineering because of their interesting mechanical and electronic properties. Their potential applications in catalysts, gas storage, nanooptical magnetic devices, and biotechnology have been extensively studied in the past decade.[1−9] Hexagonal boron nitride (*h*-BN), having hexagonal structure similar to that of graphite, consists of a regular stacking of BN honeycomb sp^2-like bonded layers. The cell parameters of *h*-BN ($a = 2.504$ Å, $c = 6.660$ Å) are close to those of graphite ($a = 2.464$ Å, $c = 6.708$ Å).[10−12] The arrangement of B and N atoms within the basal planes of BN is such that each B atom connects with three N atoms or vice versa;[13] furthermore, the bond of B−N is covalent, while the force between the planes is van der Waals force. This gives impetus to further investigate of a new branch of IF-like BN materials. Compared with graphite, boron nitride is a perfect insulator, and the IF-like BN material is a good candidate for studying low-dimensional materials in isolated environments due to its stability and heating resistance. On the basis of the local-density approximation and quasi-particle calculations, BN nanotubes are semiconductors with a uniform large gap of ∼5.5 eV (versus 5.8 eV for bulk hexagonal BN[14]) regardless of the tube diameter, chirality, and number of tube walls.[11,15] The abundant structures of BN have found potential applications in nanoscale electronic devices, ceramic materials, protective shields for encapsulated species, and hydrogen gas accumulators.[16−20] Consequently, numerous synthesis meth-

* Author to whom correspondence should be addressed. E-mail: yxielab@ustc.edu.cn.

(1) Kroto, H. W.; Heath, J. R.; O'Brien, S. C.; Curl, R. F. and Smalley, R. E. *Nature* **1985**, *318*, 162−164.
(2) Iijima, S. *Nature* **1991**, *354*, 56−58.
(3) Krishnan, A.; Dujardin, E.; Treacy, M. M. J.; Hugdahl, J.; Lynum S. and Ebbesen, T. W. *Nature* **1997**, *388*, 451−454.
(4) Ugarte, D. *Nature* **1992**, *359*, 707−709.
(5) Saito, Y.; Matsumoto, T. *Nature* **1998**, *392*, 237−237.
(6) Saito, Y.; Yoshikawa, T.; Inagaki, M.; Tomita, M.; Hayashi, T. *Chem. Phys. Lett.* **1993**, *204*, 277−282.
(7) Rao, C. N. R.; Seshadri, R.; Govindaraj, A.; Sen, R. *Mater. Sci. Eng., R* **1995**, *15*, 209−262.
(8) Oku, T.; Hirano, T.; Kuno, M.; Kusunose, T.; Niihara, K.; Suganuma, K. *Mater. Sci. Eng., B* **2000**, *74*, 206−217.
(9) Oku, T.; Kuno, M.; Kitahara, H.; Narita, I. *Int. J. Inorg. Mater.* **2001**, *3*, 597−612.
(10) Pease, R. S. *Acta Crystallogr.* **1952**, *5*, 356−361.
(11) Blase, X.; Rubio, A.; Louie, S. G.; Cohen, M. L. *Europhys. Lett.* **1994**, *28*, 335−340.
(12) Peuch, J. J., Altervitz, S. A., Eds. *Synthesis and Properties of Boron Nitride*; Matericals Science Forum; Trans Tech: Zürich, Switzerland, 1990; Vol. 54.
(13) Banhart, F.; Zwanger, M.; Muhr, H.-J. *Chem. Phys. Lett.* **1994**, *231*, 98−104.
(14) Zunger, A.; Katzir, A.; Halperine, A. *Chem. Phys. Lett.* **1976**, *13*, 5560.
(15) Chopra, N. G.; Luyken, R. J.; Cherrey, K.; Crespi, V. H.; Cohen, M. L.; Louie, S. G.; Zettl, A. *Science* **1995**, *269*, 966−967.
(16) Tang, C. C.; Bando, Y.; Ding, X. X.; Qi, S. R.; Golberg, D. *J. Am. Chem. Soc.* **2002**, *124*, 14550−14551.

10.1021/ic0348751 CCC: $27.50
Published on Web 12/18/2003

ods have been reported such as arc discharge,[15,21] electron beam irradiation,[13,22] laser ablation,[23−26] metal catalysis,[27] carbon thermal reduction,[28] the template-confined method,[29,30] the pyrolysis method,[31] the combination of ball milling and annealing,[32] chemical vapor deposition (CVD),[33−35] the copyrolysis method,[36] etc. However, the above-mentioned methods mostly used BN powders as starting materials, involved metal catalysts, or were carried out under relatively high temperatures for the synthesis of the IF-like BN nanomaterials. Herein, we demonstrate a new synthesis strategy by reacting BBr_3 with a synergic nitrogen source, $NaNH_2$ and NH_4Cl, for generating various IF-like BN structures. Some fascinating features are described in the present work: (i) BN hollow spheres are of uniform size; (ii) IF-like BN with onion structures has been successfully prepared via a solvothermal method; (iii) one kind of new nanostructure of BN, a peanut-like shape, is reported for the first time. The as-prepared IF-like BN nanostructures have been characterized with different techniques including X-ray diffraction (XRD), X-ray photoelectron spectroscopy (XPS), Fourier transform infrared (FT-IR) spectroscopy, transmission electron microscopy (TEM), high-resolution TEM (HRTEM), and field emission scanning electron microscopy (FE-SEM).

Experimental Section

Synthesis. To avoid the contamination of oxygen in air, all the manipulations were carried out in a N_2 flow glovebox. In a typical synthesis, 1.85 g (47.5 mmol) of $NaNH_2$ and 0.85 g (16.1 mmol) of NH_4Cl were added in a titanium alloy autoclave with 12 mL capacity, and then 7 mL (73.8 mmol) BBr_3 was added up to 70−80% volume. The autoclave was sealed tightly, heated at 400−450 °C for 6−12 h, and then cooled to room temperature naturally. The products were rinsed with dilute HCl solution (~1 mol·L^{-1}), followed with distilled water and acetone to remove NaBr and other impurities; finally, these gray powders were dried in a vacuum at 60 °C for 3 h.

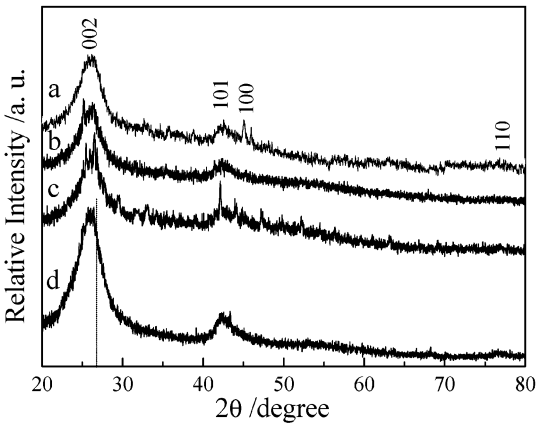

Figure 1. XRD patterns of the synthesized *h*-BN corresponding to the nanostructures of vessels (a), hollow spheres (b), peanuts (c), and onions (d).

Characterization. The composition and the structure of the as-prepared products were confirmed by the XRD pattern, using a Philip X' Pert PRO SUPER rA rotation anode with Ni-filtered Cu Kα radiation ($\lambda = 1.54187$ Å). XPS was performed on ESCALAB MKII with Mg Kα ($h\nu = 1253.6$ eV) as the excitation source. The binding energies obtained in the XPS spectral analysis were corrected for specimen charging by referencing the C_{1s} to 284.5 eV. FT-IR spectra were recorded on a Nicolet model 759 Fourier transform infrared spectrometer at wavenumbers of 500−4000 cm^{-1}. TEM images were taken with a Hitachi H-800 transmission electron microscope. The selected-area electron diffraction (SAED) patterns and HRTEM images were performed with a JEOL-2010 transmission electron microscope. FE-SEM images were taken on a field emission scanning electron microscope (JEOL JSM-6700F SEM).

Results and Discussion

Composition of the Products. The typical XRD patterns of IF-like BN with vessel, hollow sphere, peanut, and onion nanostructures are shown in Figure 1. All the reflection peaks could be indexed as hexagonal-phase boron nitride with lattice constants of $a = 2.490$ Å and $c = 6.780$ Å, which are consistent with the literature (JCPDS no. 45-895, $a = 2.504$ Å, $c = 6.656$ Å). The prominence of the (002) peak indicates the presence of well-stacked layered structures in hexagonal BN. A sharp (002) peak shown in each XRD pattern shifts slightly to a lower angle compared to that of the hexagonal BN bulk crystal. The small shifting of this peak to a lower angle indicates the lattice expansion, which could be attributed to the introduction of the strain owing to the curvature of the layers. The broadening of the (002) peak is caused by the coherent X-ray scattering of the reduced domain size in the direction that is perpendicular to the (00*l*) plane. In the lattices, the (00*l*) reflections are associated with the orderly stacking along the *c*-axis, while the (*hk*0)

(17) Chopra, N. G.; Zettl, A. *Solid State Commun.* **1998**, *105*, 297−300.
(18) Vaccarini, L.; Goze, C.; Henrard, L.; Hernandez, E.; Bernier, P.; Rubio, A. *Carbon* **2000**, *38*, 1681−1690.
(19) Srivastava, D.; Madhu, M.; Cho, K. *Phys. Rev. B* **2001**, *63*, art. No. 195413.
(20) Ma, R. Z.; Bando, Y.; Zhu, H. W.; Sato, T.; Xu, C. L.; Wu, D. H. *J. Am. Chem. Soc.* **2002**, *124*, 7672−7673.
(21) Saito, Y.; Maida, M. and Matsumoto, T. *Jpn. J. Appl. Phys., Part 1* **1999**, *38*, 159−163.
(22) Golberg, D.; Bando, Y.; Stéphan, O.; Kurashima, K. *Appl. Phys. Lett.* **1998**, *73*, 2441−2443.
(23) Boulanger, L.; Andriot, B.; Cauchetier, M.; Willaime, F. *Chem. Phys. Lett.* **1995**, *234*, 227−232.
(24) Laude, T.; Matsui, Y.; Marraud, A.; Jouffrey, B. *Appl. Phys. Lett.* **2000**, *76*, 3239−3241.
(25) Golberg, D.; Bando, Y.; Eremets, M.; Takemura, K.; Kurashima, K.; Yusa, H. *Appl. Phys. Lett.* **1996**, *69*, 2045−2047.
(26) Oku, T. *Physica B* **2002**, *323*, 357−359.
(27) Terrones, M.; Hsu, W. K.; Terrones, H.; Zhang, J. P.; Ramos, S.; Hare, J. P.; Castillo, R.; Prassides, K.; Cheetham, A. K.; Kroto, H. W.; Waltor, D. R. M. *Chem. Phys. Lett.* **1996**, *259*, 568−573.
(28) Pokropivny, V. V.; Skorokhod, V. V.; Oleinik, G. S.; Kurdyumov, A. V.; Bartnitskaya, T. S.; Pokropivny, A. V.; Sisonyuk, A. G.; Sheichenko, D. M. *J. Solid State Chem.* **2000**, *154*, 214−222.
(29) Han, W. Q.; Bando, Y.; Kurashima, K.; Sato, T. *Appl. Phys. Lett.* **1998**, *73*, 3085−3087.
(30) Shelimov, K. B.; Moskovits, M. *Chem. Mater.* **2000**, *12*, 250−254.
(31) O. R. Lourie, C. R. Jones, Bartlett, B. M.; Gibbons, P. C.; Ruoff, R. S.; Buhro, W. E. *Chem. Mater.* **2000**, *12*, 1808−1810.
(32) Chen, Y.; Chadderton, L. T.; FitzGerald, J.; Williams, J. S. *Appl. Phys. Lett.* **1999**, *74*, 2960−2962.
(33) Ma, R. Z.; Bando, Y.; Sato, T.; Kurashima, K. *Chem. Mater.* **2001**, *13*, 2965−2971.
(34) Ma, R. Z.; Bando, Y.; Sato, T. *Adv. Mater.* **2002**, *14*, 366−368.
(35) Tang, C. C.; Bando, Y.; Sato, T.; Kurashima, K. *Chem. Commun.* **2002**, 1290−1291.
(36) Xu, L. Q.; Peng, Y. Y.; Meng, Z. Y.; Yu, W. C.; Zhang, S. Y.; Liu, X. M.; Qian, Y. T. *Chem. Mater.* **2003**, *15*, 2675−2680.

reflections indicate the ordering in the basal *ab* planes. From the XRD patterns, an expansion (ca. 2−4%) along the *c*-axis could be observed in the as-synthesized IF-like BN materials. These characteristics are considered as some of the evidence for the formation of fullerene-like particles.[39−42] No other noticeable peaks introduced by impurities are observed in the XRD patterns (Figure 1).

The composition of the as-prepared *h*-BN could be derived from the XPS spectra (shown in Figure 2). Figure 2a is a typical survey spectrum of the IF-like *h*-BN with vessel structures, indicating the presence of B and N elements. The appearance of other impurity peaks is due to the adsorption of CO_2 and O_2 onto the surface of the sample. The binding energies centered at 190.55 eV for B_{1s} (Figure 2b) and 398.25 eV for N_{1s} (Figure 2c) are in good agreement with the values of bulk BN in the literature.[43] The average atomic ratio of B to N is around 1.037:1 on the basis of the quantification of the B_{1s} and N_{1s} peaks. Another three *h*-BN samples with atomic ratios of 1.019:1, 1.114:1, and 1.138:1 were also prepared at 400 °C for 9 h, 400 °C for 12 h, and 450 °C for 6 h, respectively. Figure 3 shows a series of typical FT-IR spectra of IF-like *h*-BN with vessel, hollow sphere, peanut, and onion structures, respectively, in which two strong characteristic peaks positioned at ∼1385 and ∼800 cm^{-1} are observed. The peak centered at ∼1385 cm^{-1} should result from the in-plane B−N TO models of the sp^2-bonded *h*-BN, while the absorption band at ∼800 cm^{-1} could be attributed to the B−N−B bonding vibration out of the plane.[44] The broad absorption peak at ∼3420 cm^{-1} is caused by the absorption of H_2O in air. On the basis of the above characterizations of XRD patterns and XPS and FT-IR spectra, the as-synthesized products are pure-phase *h*-BN.

Morphologies and Structures. TEM, HRTEM and FE-SEM images of the as-prepared *h*-BN are shown in Figures 4−7, respectively. Parts a and b of Figure 4 show the typical TEM images of *h*-BN with vessel structures prepared at 400 °C for 6 h. The proportion of the product with vessel structures is as high as 40−50%. The diameter of the BN vessels is in the range of 120∼240 nm, and the length of the vessels varies from 0.6 to 2.4 μm; some rectangularly bent vessels can be found in the sample (Figure 4b). The coexistence of a vessel and a curling sheet can also be observed in Figure 4c. A typical SAED pattern from the base of the BN vessels is shown as the inset of Figure 4b and exhibits some elongated diffraction spots as well as discontinuous rings rather than full rings, which indicate the BN vessels are polycrystallites with their growth orientation mainly concentrated on a certain direction. Figure 4d is an HRTEM image of the BN vessel, which shows the fringe stacking of the vessel wall. The interspace between two adjacent layers is around 0.34 nm, consistent with the interplane distance of 0.333 nm in bulk *h*-BN.[10,45] A typical EDXA pattern (Figure 4e) shows BN vessels are composed of elemental B and N. The energy peaks of Cu and O are

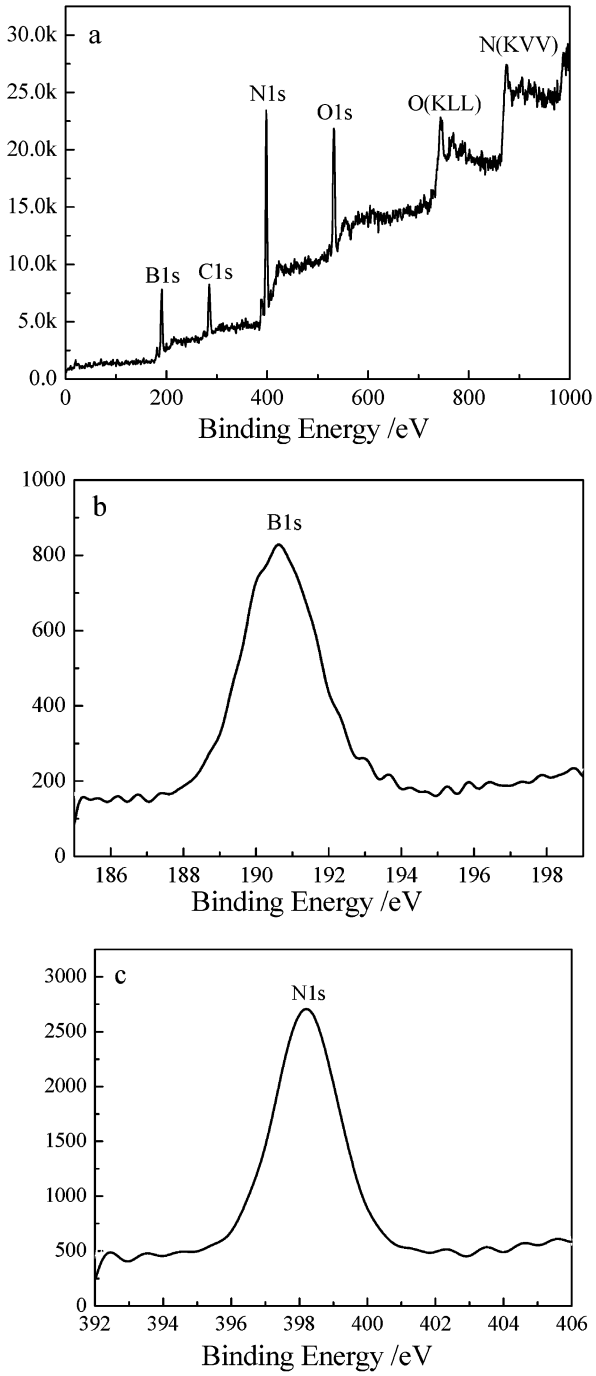

Figure 2. XPS spectra of *h*-BN with vessel structures: (a) survey spectrum; (b) B_{1s} region; (c) N_{1s} region.

(37) Bai, X. D.; Zhong, D. Y.; Zhang, G. Y.; Ma, X. C.; Liu, S.; Wang, E. G.; Chen, Y.; Shaw, D. T. *Appl. Phys. Lett.* **2001**, *79*, 1552−1554.
(38) Feldman, Y.; Lyakhovitskaya, V.; Tenne, R. *J. Am. Chem. Soc.* **1998**, *120*, 4176−4183.
(39) Homyonfer, M.; Alperson, B.; Rosenberg, Y.; Sapir, L.; Cohen, S. R.; Hodes, G.; Tenne, R. *J. Am. Chem. Soc.* **1997**, *119*, 2693−2698.
(40) Feldman, Y.; Frey, G. L.; Homyonfer, M.; Lyakhovitskaya, V.; Margulis, L.; Cohen, H.; Hodes, G.; Hutchison, J. L.; Tenne, R. *J. Am. Chem. Soc.* **1996**, *118*, 5362−5367.
(41) Chhowalla, M.; Amaratunga, G. A. J. *Nature* **2000**, *407*, 164−167.
(42) Wagner, C. D., Riggs, W. W., Davis, L. E., Moulder, J. F., Muilenberg, G. E., Eds. *Handbook of X-ray Photoelectron Spectroscopy*; Physical Electronics Division, Perkin-Elmer Corp.: Eden Prairie, MN, 1979.
(43) Tang, C. C.; Bando, Y.; Sato, T.; Kurashima, K. *Adv. Mater.* **2002**, *14*, 1046−1049.
(44) Paine, R. T.; Narula, C. K. *Chem. Rev.* **1990**, *90*, 73−91.
(45) Geyer, W.; Stadler, V.; Eck, W.; Zharnikov, M.; Gölzhäuser, A.; Grunze, M. *Appl. Phys. Lett.* **1999**, *75*, 2401−2403.

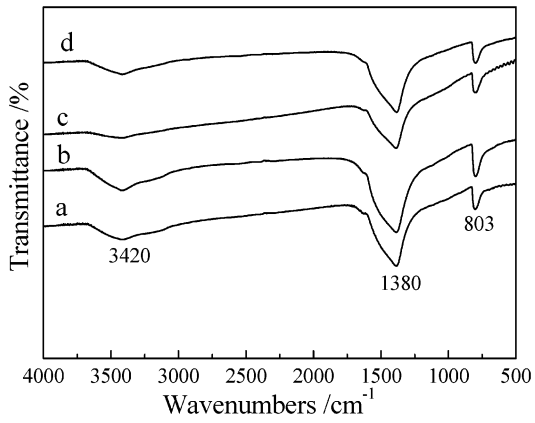

Figure 3. FT-IR spectra of the obtained *h*-BN corresponding to the nanostructures of vessels (a), hollow spheres (b), peanuts (c), and onions (d).

derived from the copper grid and the absorption of oxygen in air. Figure 4f displays a panoramic FE-SEM image of the product and exhibits its vessel-like morphology, in which most of the vessels are not straight and have open ends. This is consistent with the corresponding TEM studies.

Hollow spheres of boron nitride were prepared at 400 °C for 9 h, and the proportion of the hollow spheres occupies about 20−30%. The TEM image (Figure 5a) shows the hollow nature on the basis of a strong contrast between the dark edge and pale center.[46] It is evident that the boundary of the shells is well defined and some hollow spheres are aligned together. The outer diameter of the hollow spheres is around 300 nm, and the average thickness of the shells is ∼60 nm. The inset in Figure 5a shows the SAED pattern of the BN hollow spheres, in which the intense diffraction rings can be indexed to the (002) and (100) planes of *h*-BN nanocrystals from inner to outer, respectively. In addition, segmented vessels and some quasi-hollow spheres could be found in the final product as shown in Figure 5b. Figure 5c is an HRTEM image of a portion of the BN hollow sphere, revealing that the shell is composed of layers and the interspace distance is about 0.34 nm. The hollow nature could be further confirmed by some broken hollow spheres shown in the FE-SEM image (Figure 5d).

Parts a and b of Figure 6 show TEM images and the typical SAED pattern of the as-prepared products heated at 400 °C

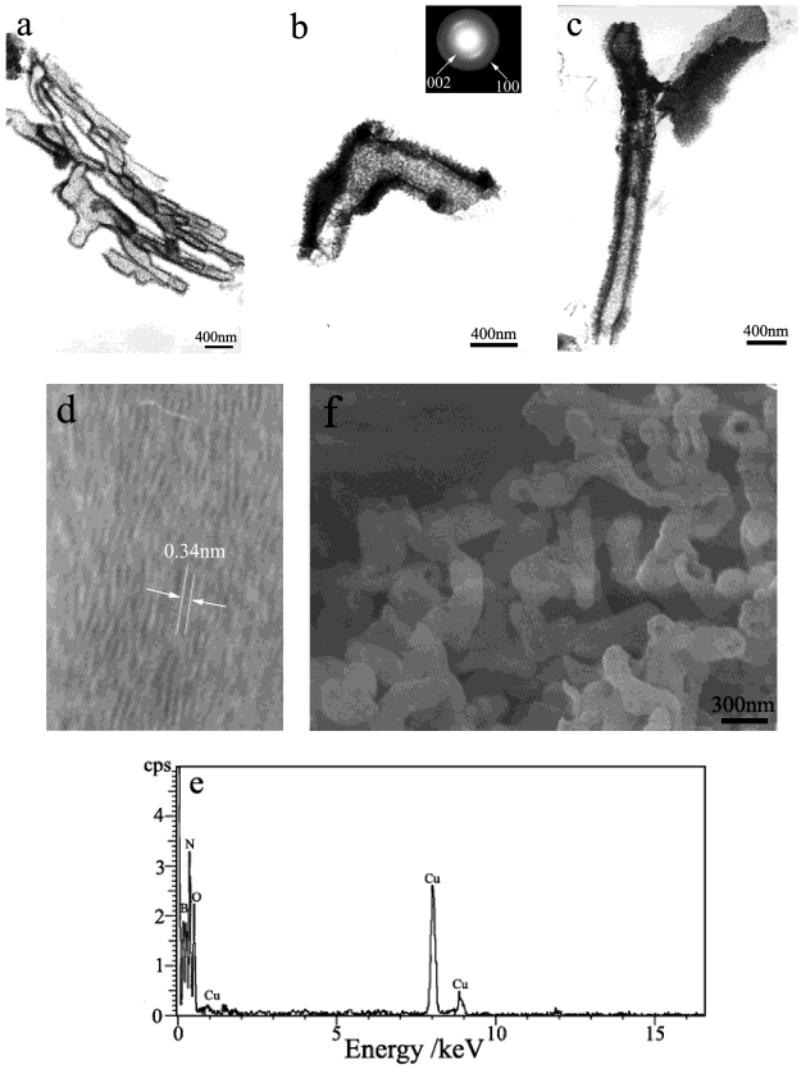

Figure 4. (a) A typical TEM image of the as-prepared *h*-BN vessels. (b) A TEM image showing a rectangular vessel of BN with the inset corresponding to the SAED pattern. (c) A TEM image showing the coexistence of the BN vessel and the curling sheet. (d) An HRTEM image and (e) the EDXA pattern of *h*-BN vessels. (f) An FE-SEM image of BN vessels with open ends.

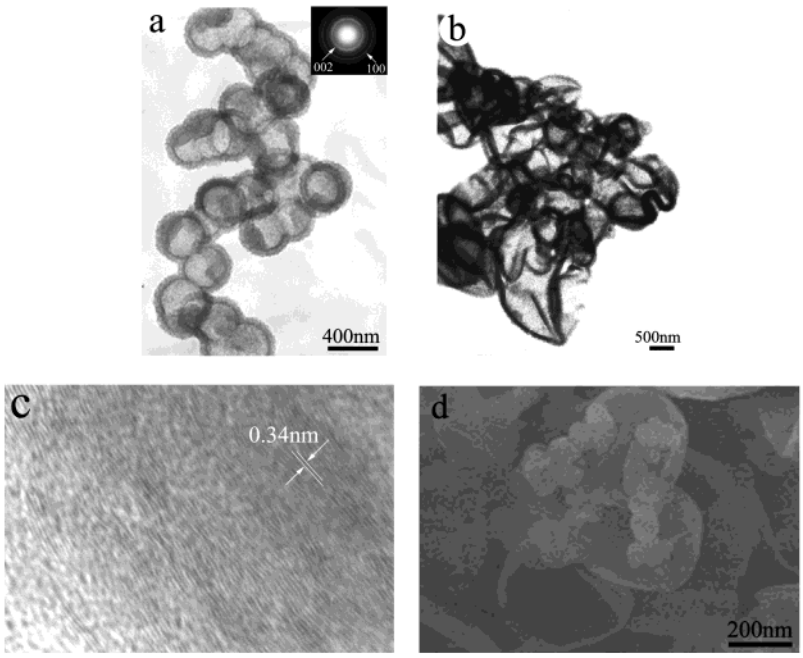

Figure 5. (a) A typical TEM image of the as-prepared *h*-BN hollow spheres with a well-defined boundary (the inset is the SAED pattern of the BN hollow spheres). (b) A TEM image showing the coexistence of the segmented vessels and quasi-hollow spheres. (c) An HRTEM image of *h*-BN hollow spheres. (d) An FE-SEM image confirming the hollow nature of the spheres.

for 12 h. This sample is mainly made up of peanut-like structures together with a small amount of hollow spheres. Apparently, space exists between the core and shell in the peanut-like structures. The yield of nanopeanuts is ∼40% estimated from the TEM images. The diameter of the shell is 200∼250 nm and that of the core around 120∼150 nm with the interstice of 30−40 nm in the *h*-BN nanopeanuts. The boundary of the shell is well distinguished, and the self-encapsulated structures could be observed in the form of either a single core or twins. The doublet shown in Figure 6b is highly reminiscent of peanut-like structure. The inset of Figure 6a shows the SAED pattern of the BN nanopeanuts, indicating that the shell of BN peanuts consisted of hexagonal BN polycrystallites. In addition, we also observe that the compressed hollow spheres tend to be onion-like structures with a size of 120∼160 nm (Figure 6c). The diameter of the coexistent onion-like particles is close to that of the peanut core. Figure 6d displays an HRTEM image of the BN nanopeanuts, showing the interstice between the core and shell is about 30−40 nm. Figure 6e reveals the typically coexistent onion-like structures, which exhibit clearly that the onion-like shell is composed of around 9−15 layers. The peanut structures are also confirmed by the FE-SEM images of the twin spheres (Figure 6f) and a half-broken peanut of BN (Figure 6g).

The TEM images (Figure 7a,b) of the product prepared at 450 °C for 6 h show that the onion-like structures are dominant with the coexistence of a few peanuts. The yield of onion-like *h*-BN and that of peanut-like *h*-BN are ∼30% and ∼10%, respectively. The diameter of the onions is ∼260−300 nm, which is close to the size of the peanuts. Several diffraction rings in a typical SAED pattern (inset of Figure 7b) could be indexed to the (002) and (100) planes of the hexagonal BN structures. Figure 7c shows an HRTEM image of *h*-BN with onion-like structures. In contrast to the small onion-like BN particles in Figure 6e, the core of the larger onion-like structures is almost amorphous and the lattice fringes of the core can hardly be observed, which is similar to the phenomenon previously reported.[13] Apparently, the small BN onions preferentially exhibit the curled layers whereas the larger ones tend to arrange themselves in disordered planar units.[13]

Formation Mechanism of *h*-*BN*. Our approach to *h*-BN nanostructures is essentially based on the liquid−solid reaction between BBr_3 and the synergic nitrogen sources $NaNH_2$ and NH_4Cl. It is well-known that $NaNH_2$ could decompose to Na_3N by loss of ammonia on heating[47] and NH_4Cl could also decompose to NH_3 on heating, as described in the following eqs 1 and 3. The freshly produced Na_3N and NH_3 could be regarded as the intermediate reactants and instantly react with BBr_3 to form *h*-BN nanocrystals, as described in eqs 2 and 4. One direct evidence for NH_3 participating in the reaction as one of the nitrogen sources is that no offensive odor of NH_3 can be detected when the autoclave is opened after the reaction is fully quenched. Additionally, the byproducts HX (X = Cl, Br) in this approach could provide the non-oxygen environment in the sealed system. From the thermodynamic point of view, the reaction between BBr_3 and $NaNH_2$ is described as eqs 1 and 2 and is thermodynamically driven to the right side and highly exothermic ($\Delta G_f^\circ = -877.70$ kcal·mol^{-1}, $\Delta H_f^\circ = -818.12$ kcal·mol^{-1}),[48] while the reaction between BBr_3 and NH_4Cl, described as eqs 3 and 4 is thermodynamically driven to the right side and endothermic ($\Delta G_f^\circ = -34.78$ kcal·mol^{-1}, $\Delta H_f^\circ = 79.78$ kcal·mol^{-1}).[48] The coformation of alkali-metal halide (here NaBr) accounts for up to 90% of the enthalpy

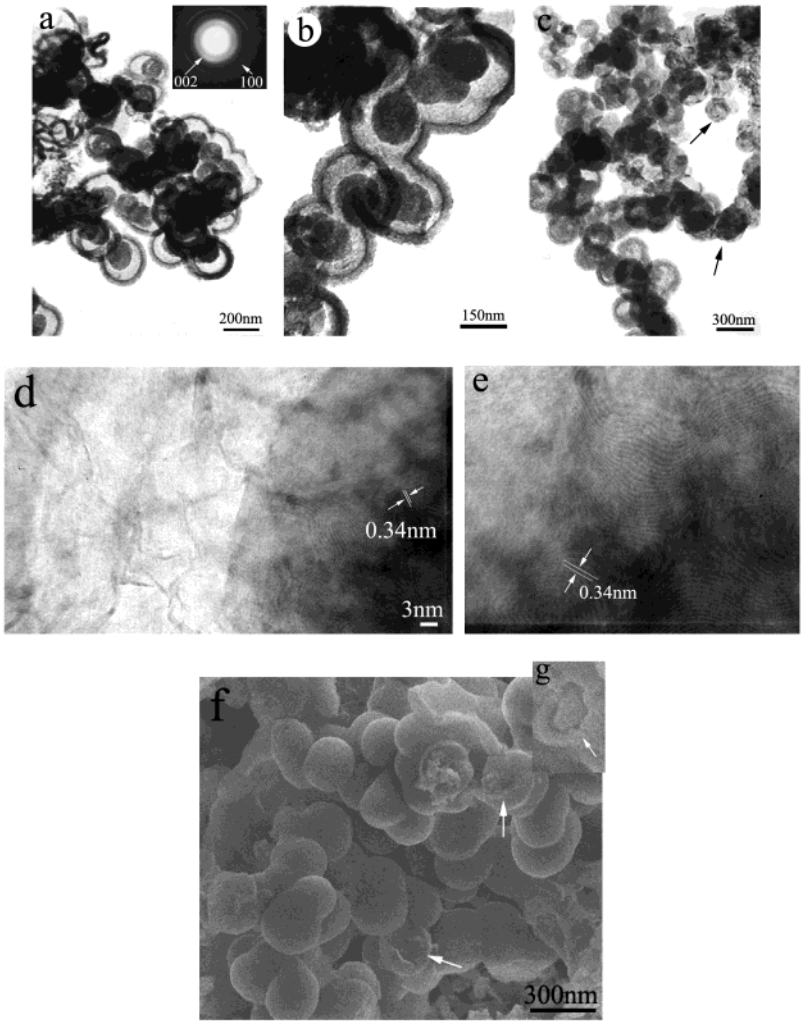

Figure 6. (a) A typical TEM image of the as-obtained *h*-BN peanut structures (the inset corresponds to the SAED pattern of the BN nanopeanuts). (b) A TEM image showing the BN nanopeanuts with either a single core or twins. (c) A TEM image showing the coexistence of nanopeanuts and some quasi-onions of BN. (d) An HRTEM image of *h*-BN nanopeanuts with an interplane distance of 0.34 nm. (e) A typical HRTEM image of compressed spheres directed by the arrow in Figure 6c clearly showing the existence of BN onion structures. (f) An FE-SEM image of BN nanopeanuts showing the twin BN spheres and some broken spheres. (g) An FE-SEM image exhibiting a broken peanut.

of reaction (eq 2).[49,50] The heat produced in the reaction in eq 2 is sufficiently exothermic and could be transferred to the reaction in eq 4, which not only prevents the products from sintering but also guarantees the reaction in eq 4 proceeds smoothly. The total reaction could be described by eq 5. In our experiments, the products were amorphous *h*-BN if the single nitrogen source, either $NaNH_2$ or NH_4Cl, was used even though the temperature was increased to 500 °C. It is the synergic effect of the two nitrogen sources that results in the formation of polycrystalline *h*-BN nanostructures at relatively lower temperatures (400−450 °C), and this validity of the synergic nitrogen source has been demonstrated in our previous work.[51]

$$3NaNH_2 \rightarrow Na_3N + 2NH_3 \quad (1)$$

$$BBr_3 + Na_3N \rightarrow h\text{-}BN + 3NaBr \quad (2)$$

$$NH_4Cl \rightarrow NH_3 + HCl \quad (3)$$

$$BBr_3 + NH_3 \rightarrow h\text{-}BN + 3HBr \quad (4)$$

$$\Rightarrow 4BBr_3 + 3NaNH_2 + NH_4Cl \rightarrow 4h\text{-}BN + 3NaBr + 9HBr + HCl \quad (5)$$

Growth Mechanism of IF-like *h-BN with Vessel, Hollow Sphere, Onion, and Peanut Structures.* The structure of *h*-BN is similar to that of graphite, and the appearance of these artistic structures such as vessels, hollow spheres, onions, and peanuts is basically determined by the layer structures of *h*-BN. Under certain conditions, the interaction of the lamellar interlayers could be diminished from the edges and the rolling process could proceed. The sealed system with high pressure is also helpful for the rolling of the sheets, which is similar to the graphite layers curled with the assistance of various driving forces. Heidenreich et al. have

(46) Tenne, R., Karlin, K. D., Eds. *Progress in Inorganic Chemistry*; John Wiley & Sons: New York, 2002; Vol 50, pp 269−315.
(47) Cotton, F. A., Wilkison, G., Murillo, C. A., Bochmann, M., Eds. *Advanced Inorganic Chemistry*; John Wiley & Sons: New York, 1999.
(48) Dean, J. A., Ed. *Lange's Handbook of Chemistry*, 13th ed.; McGraw-Hill: New York, 1985.
(49) Parkin, I. P. *Chem. Soc. Rev.* **1996**, *25*, 199−209.
(50) Gillan, E. G.; Kaner, R. B. *Chem. Mater.* **1996**, *8*, 333−343.
(51) Xu, F.; Zhang, X.; Xi, W.; Hong, J.; Xie, Y. *Chem. Lett.* **2003**, *32*, 600−601.

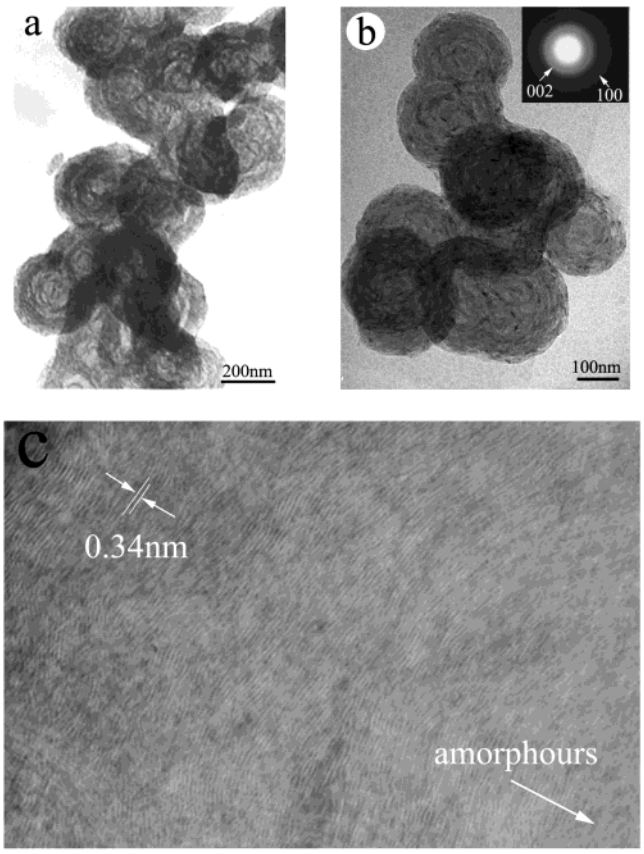

Figure 7. (a) A TEM image of the as-prepared *h*-BN onions. (b) A TEM image showing the twin structures of BN onions (the inset is the SAED pattern of the BN onions). (c) A typical HRTEM image of large *h*-BN onions in which the core of the large onion structures is nearly amorphous (as the arrow directs).

investigated that the severe bonding of graphite sheets commonly occurs at high temperatures.[52] In addition, the curling of graphitic networks could be observed under electron beam irradiation.[4] All these studies give us the inspiration that the possibility of the rolling process of the lamellar *h*-BN structures exists in the sealed system with high pressure and temperature. The coexistence of a vessel and a curling sheet (Figure 4c) is direct evidence for this rolling process. With increasing reaction time, the BN vessels seem to be unstable and are apt to form segmental BN vessels, and some quasi-hollow spheres formed are shown in Figure 5b. Ma et al. reported the appearance of BN nanotubes and nanobamboos by using the CVD method,[34] in which a kind of metastable growth condition would prevent the growth of cylindrical tubes and some tubular layers would tend to close up and thus form the segmented nanobamboos. As for the reaction conditions in this work, the high pressure coming from NH_3 and HX in the sealed system may provide a kind of metastable growth condition. Therefore, the vessels are tentative to close up to minimize their surface energy, leading to the formation of the segmented vessels. The segmented vessels and quasi-hollow spheres, as shown in Figure 5b, possibly form the final hollow spheres. Furthermore, the layer nature of *h*-BN hollow spheres (Figure 5c) indicates that the vessels close up to form hollow spheres and still maintain the layer structures. When the reaction time is increased to 12 h, some hollow spheres seem to be compressed into small onions and self-encapsulate into another kind of larger hollow sphere, forming the BN nanopeanuts. This is the possible reason that the onion-like structures are observed with the coexistence of peanut-like BN structures (Figure 6f,g). The formation of the closed onion structures could saturate the dangling bonding and lead to an energy decrease of the system.[53,54] When the reaction time is more than 12 h with keeping the reaction temperature at 400 °C, there is no further influence on the morphology of *h*-BN. When the temperature is increased to 450 °C and the reaction time is kept at 6 h, the amount of the peanuts decreases and that of the onions increases. That is, when the reaction temperature is kept at 400 °C while the reaction time is increased from 6 to 9 and 12 h, the structures of BN transform from vessels to hollow spheres to peanuts. When the reaction time is kept at 6 h while the reaction temperature is increased from 400 to 450 °C, the BN structures change from vessels to onions. It is apparent that the reaction temperature has a more prominent effect on the structures of *h*-BN than the reaction time, perhaps involving the pressure produced abruptly at the initial stage of the reaction. The higher temperatures or the longer times are useful for the formation of the closed structures, while the lower temperatures or the shorter times favor the formation of the vessels. On the other hand, when nanoclusters of 2H compounds are formed, the prismatic edges are decorated with dangling bonds, having stored enough chemical energy to destabilize the planar structures. In the absence of the reactive chemical species (i.e., H_2O, O_2), an alternative mechanism for the annihilation of the peripheral dangling bonds may be raised, which leads to the formation of hollow nanostructures. For this process to take place, sufficient thermal energy and pressure are required to overcome the activation barriers associated with the bending of the layers (elastic strain energy).[52] In this case, the stable hollow nanostructures are fabricated in the form of vessels, hollow spheres, onions, and peanuts, respectively. The synergic nitrogen sources, the reaction temperature, and the reaction time are vital for controlling nanostructures in this sealed system. And this may be a perfect example produced by the nanoscale self-assembly.

Conclusions

In summary, fullerene-like *h*-BN with vessel, hollow sphere, onion, and peanut structures has been synthesized via a synergic nitrogen source route involving the liquid−solid reaction of BBr_3 with the synergic nitrogen sources $NaNH_2$ and NH_4Cl at 400−450 °C for 6−12 h. This is a successful example of the preparation of *h*-BN with vessel, hollow sphere, peanut, and onion-like structures via this

(52) Heidenteich, R. D.; Hess, W. M.; Ban, L. L. *J. Appl. Crystallogr.* **1968**, *1*, 1−19.
(53) Saito, R.; Fujita, M.; Dresselhaus, G.; Dresselhaus, M. S. *Phys. Rev. B* **1992**, *46*, 1804−1811.
(54) Iijima, S. *MRS Bull.* **1994**, 43−49.

solvothermal method; especially the synthesis of *h*-BN with peanut structures is reported for the first time here. Combined with the TEM and HRTEM images, the possible formation mechanism has been discussed. Moreover, IF-like *h*-BN with vessel, hollow sphere, peanut, and onion structures may have a higher gravimetric hydrogen uptake capacity, which may be advantageous in the gas storage applications. This self-assembly process in a sealed system may be extended to prepare other inorganic fullerene-like materials with more abundant nanostructures.

Acknowledgment. Financial support from the National Natural Science Foundation of China, Chinese Ministry of Education, and Chinese Academy of Sciences is gratefully acknowledged.

IC0348751